Available online at www.sciencedirect.com

SCIENCE DIRECT

Developmental Biology 294 (2006) 168–180

DEVELOPMENTAL BIOLOGY

www.elsevier.com/locate/ydbio

A subpial, transitory germinal zone forms chains of neuronal precursors in the rabbit cerebellum

Giovanna Ponti [a], Paolo Peretto [b], Luca Bonfanti [a,c,*]

[a] *Department of Veterinary Morphophysiology, University of Turin, Via Leonardo da Vinci 44, 10095 Grugliasco, Italy*
[b] *Department of Animal and Human Biology, University of Turin, Via Accademia Albertina 13, 10153 Turin, Italy*
[c] *Rita Levi Montalcini Center for Brain Repair, Italy*

Received for publication 3 January 2006; revised 20 February 2006; accepted 22 February 2006
Available online 3 April 2006

Abstract

Protracted neurogenesis occurs at different postnatal stages in different brain locations, whereby leading to site-specific adult neurogenesis in some cases. No spontaneous genesis of neurons occurs in the cerebellum after the postnatal genesis of granule cells from the external germinal layer (EGL), a transitory actively proliferating zone which is thought to be exhausted before puberty. Here, we show the protracted genesis of newly generated neuronal precursors in the cerebellar cortex of young rabbits, persisting beyond puberty. Neuroblasts generated within an actively proliferating subpial layer thus extending the postnatal EGL are arranged to form thousands of tangential chains reminiscent of those responsible for cell migration in the forebrain subventricular zone. These subpial chains cover the whole cerebellar surface from the 2nd to the 5th month of life, then disappearing after puberty. In addition, we describe the appearance of similar groups of cells at the end of granule cell genesis in the mouse cerebellum, here limited to the short period of EGL exhaustion (4–5 days). These results show common features do exist in the postnatal reorganization of secondary germinal layers of brain and cerebellum at specific stages, parallel to differences in the slowing down of cerebellar neurogenesis among mammalian species.

Keywords: Development; Neurogenesis; Migration; Meninges; PSA-NCAM

Introduction

Adult neurogenesis persists throughout life in two restricted brain areas: the dentate gyrus of the hippocampus and the forebrain subventricular zone (SVZ) (Gage, 2000; Alvarez-Buylla and Garcia-Verdugo, 2002). Unlike the forebrain, the mammalian cerebellum is considered incapable of any spontaneous cell genesis after the exhaustion of the external germinal layer (EGL). The EGL is a secondary actively proliferating zone made up of cell precursors which originate from the germinal trigone following tangential subpial displacement (Altman and Bayer, 1997), then leading to delayed genesis of the granule cell population in the postnatal developing cerebellar cortex. In all species studied, this transitory germinal zone is formed by several layers of granule cell precursors which progressively reduce their thickness as the cells migrate deep into the cortex to form the inner granule layer (GL). In atricial mammals (Sanchez-Villagra and Sultan, 2001), the EGL is active in the pre- and postnatal period, then disappearing parallel to or before accomplishing postnatal granule cell genesis, which occurs at specific ages: postnatal day 21 in mice (Fujita et al., 1966) and 22 in rats (Altman, 1969), postnatal month 3 in primates (Rakic, 1971) and 11 in humans (Abraham et al., 2001). After EGL exhaustion, direct contact between the pial surface and Bergmann glial endfeet on one side and parallel fibers on the other is thought to characterize the external part of the molecular layer (ML) (Altman and Bayer, 1997). Although in rabbits the end of cell genesis and the neurochemical maturation of the

Abbreviations: SVZ, subventricular zone; PSA-NCAM, polysialylated neural cell adhesion molecule; BrdU, 5-bromo-2′-deoxyuridine; ML, molecular layer; GL, inner granular layer; EGL, external germinal layer; SPL, subpial layer; DCX, doublecortin; CNS, central nervous system.

* Corresponding author. Dip. di Morfofisiologia Veterinaria, Via Leonardo da Vinci, 44, 10095-Grugliasco (TO) Italy. Fax: +39 011 6709138.
E-mail address: luca.bonfanti@unito.it (L. Bonfanti).

0012-1606/$ - see front matter © 2006 Elsevier Inc. All rights reserved.
doi:10.1016/j.ydbio.2006.02.037

cerebellum have been fixed around the second postnatal month (Smith, 1963; Lossi et al., 1995), here, we describe the existence of a secondary germinal matrix persisting beyond puberty in subpial position. This subpial layer originating from a structural modification of the EGL is capable of generating neuronal precursors which assemble to form tangential chains reminiscent of the forebrain SVZ, namely the main adult neurogenetic area of the mammalian brain (Gage, 2000; Alvarez-Buylla and Garcia-Verdugo, 2002). In addition, since rodents and lagomorphs belong to distinct mammalian orders, we have studied the last phases of mouse EGL revealing a tendency to form chain-like structures similar to rabbit SPL chains, here restricted to a very short period in coincidence with the exhaustion of the germinative layer.

Materials and methods

5-Bromo-2′-deoxyuridine (BrdU) injections and tissue preparation

Experimentation was conducted in accordance with current EU and Italian laws (Italian Ministry of Health, authorization n. 66/99-A). Twenty-two peripuberal (3–5 months old; Charles River, Milan) New Zealand White rabbits (*Orictolagus cuniculus*) were used for light microscopy. Seventeen received intraperitoneal injections of BrdU (Sigma; 40 mg/kg). Eight received a single injection, five were killed after 2 h and three after 5 days. Nine rabbits received one daily injection for 5 days and were killed 2 h, 5 and 10 days (n = 3 each) after the last injection. In addition, two 4-month-old rabbits for electron microscopy, two 6-month-old and four adult (1 and 2 year old) rabbits for light microscopy, were used. Twelve postnatal rabbits (10, 15, 23, 30, 40, 75 days old) were treated with BrdU for 2 h. Cerebella from 18 young (P15, P18, P21, P24, P26; P28; n = 3 for each age) CD-1 mice (Charles River, Italy) were also used for light microscopy. In addition, two P21 mice were used for electron microscopy.

Animals were anesthetized with a ketamine/xylazine solution (100 mg/kg body weight: 33 mg/kg body weight) and perfused as previously described (Luzzati et al., 2003; Peretto et al., 2005). Cerebella were extracted carefully to preserve the pia mater, postfixed 6 h (light microscopy), frozen at −80°C and cryostat (16 μm thick) or vibratome (100 μm thick) sectioned in series, along sagittal and coronal orientation. Tissues for electron microscopy were postfixed 2 h, cut sagittally using a blade (about 300 μm thick), then fixed in osmium-ferrocyanide for 1 h, stained en bloc with 1% uranyl acetate, dehydrated, embedded in Araldite and processed as previously described (Luzzati et al., 2003). Ultra-thin sections were examined with a Philips CM10 transmission electron microscope. Semithin sections for light microscopy (1 μm thick) were stained with 1% toluidine blue and 0.5% $NaHCO_3$.

Immunohistochemistry

Immunohistochemical reactions were carried out by using single peroxidase and double immunofluorescence methods on cryostat sections incubated overnight at room temperature with primary antibodies: (i) anti-BrdU, 1/600 (monoclonal, Harlan Laboratories, Haslett, MI); (ii) anti-Ki67, 1/300 (MIB1, monoclonal, Immunotech, Luminy); 1/2000 (polyclonal, Novocastra); (iii) anti-laminin, 1/200 (polyclonal, Chemicon); (iv) anti-PSA-NCAM, diluted 1/3500 (monoclonal IgM; G. Rougon, Marseille, France); (v) anti-class III β-tubulin, 1/1000 (TU-J1, monoclonal and polyclonal, Babco, Richmond, VA); (vi) anti-human neuronal protein HuC/D, 1/200 (monoclonal, Molecular Probes); (vii) anti-DCX, 1/750 (polyclonal goat, Santa Cruz); (viii) anti-glial fibrillary acidic protein, 1/1000 (GFAP, polyclonal, DAKO); (ix) anti-vimentin, 1/800 (monoclonal, DAKO); (x) anti-Ng2 chondroitin sulfate proteoglycan, 1/250 (polyclonal, Chemicon); anti-O4, 1/200 (monoclonal, Chemicon). All polyclonal antisera used did not give any problem on the rabbit cerebellar tissue. For double staining, indirect immunofluorescence procedures using FITC–avidin + Cy3 conjugated antibodies were used. Antibodies were diluted in 0.01 M PBS, pH 7.4, containing 0.5% Triton X-100. Fluorescent specimens mounted in 1,4-diazabicyclo[2.2.2]octane (Dabco, Sigma) were observed with a laser scanning Olympus Fluoview confocal system.

Electron microscopic serial reconstructions

The electron microscopic reconstruction of two rabbit SPL chains was carried out on serial ultra-thin sections (80 nm thick) collected onto Formvar-coated grids. Micrographs from the sixth section in the sequence were drawn to define the contour of single cells and processes. The digital images have been added in sequence on Adobe Photoshop software. Drawings from 43 levels were examined to follow the behavior of the chain across a total length of 21 μm. The reconstruction of a mouse subpial chain-like structure was performed using the same method, although in this case the drawing of one section every 12 (about 1 μm interval) was enough, due to the presence of a small number of cell processes. A total of 16 sections, up to a total length of 16 μm, were considered.

Cell countings and statistical analysis

The amount of newly generated cells in the cerebellum of 12 3-month-old rabbits was analyzed by counting the number of BrdU-immunoreactive nuclei in parasagittal cryostat sections, at 2 h (animals n = 3), 5 (n = 6: 3 after a single injection, 3 after 5 injections) and 15 (n = 3 after 5 injections) days survival times. A total of 200 mm of pial surface and underlying cortex was analyzed in 3 representative sections for each animal, cut at different medial–lateral levels. Immunoreactive nuclei present on the cerebellar surface (cut nuclei were considered only on one side of the section) and in cerebellar cortical layers (on a single focal plane) were counted. Images of the cortical areas were imported on Image proplus, then countings of total nuclei, nuclei densities and nuclei/number of cells (on cresyl violet-stained sections) were performed in the SPL (5 μm beneath the pial surface), ML and GL. Parallel sections were used to estimate the percentage of BrdU/PSA-NCAM double-labeled cells detectable in the SPL at 2 h and 5 days survival times (total cells counted = 7291).

The number of proliferating cells in each cerebellar layer has been analyzed by one-way ANOVA with main factor time and repeated measurements factor of layer (SPL, ML, GL). Statistical analyses of data were performed by the SPSS statistical software (version 12.01 for Windows). A value of $P \leq 0.05$ was accepted as statistically significant.

The number of PSA-NCAM-immunoreactive cells in each layer was counted in an area corresponding to 10 mm of pial surface in representative thick vibratome sections (animals n = 3; total cells counted = 6341). In the SPL, due to the presence of chains, 2 bipolar cells/chain were considered.

Results

A proliferative layer persists in the young rabbit cerebellum

By using endogenous (Ki67 antigen) and exogenously administered (5-bromo-2′-deoxyuridine, BrdU) markers of cell proliferation a consistent amount of newly generated cells were found in the cerebellar cortex of peri-puberal (3- to 5-month-old) rabbits (Fig. 1). BrdU detected at 2-h survival time was used to identify s-phase cells, and Ki67 confirmed this labeling as cell proliferation and not DNA repair (Kee et al., 2002; Rakic, 2002). In BrdU/Ki67 double labelings, both antigens were concentrated at the same sites, all BrdU+ cells resulting double-stained. As expected, Ki67 revealed a higher number of cells (Fig. 1A), due to its estimated permanence in the cell cycle (Kee et al., 2002). Most proliferating cells were observed along the cerebellar surface (Fig. 1). Double stainings for proliferation markers and laminin (Fig. 1B), and semithin sections from resin-embedded material (Fig. 1C) showed that the vast majority of proliferating elements occupied a specific subpial position, which did not affect the meninges. Dividing

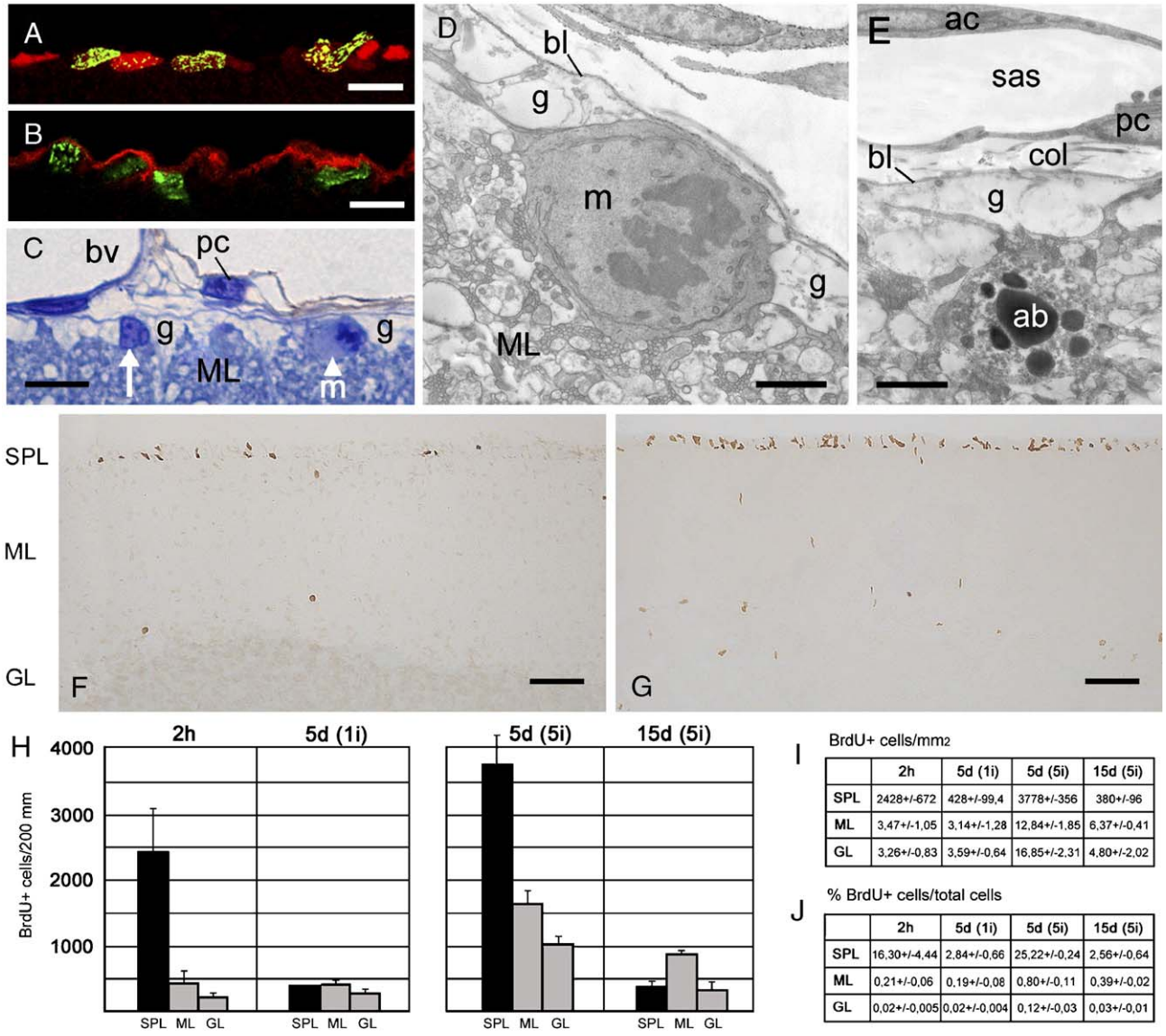

	2h	5d (1i)	5d (5i)	15d (5i)
SPL	2428+/-672	428+/-99,4	3778+/-356	380+/-96
ML	3,47+/-1,05	3,14+/-1,28	12,84+/-1,85	6,37+/-0,41
GL	3,26+/-0,83	3,59+/-0,64	16,85+/-2,31	4,80+/-2,02

	2h	5d (1i)	5d (5i)	15d (5i)
SPL	16,30+/-4,44	2,84+/-0,66	25,22+/-0,24	2,56+/-0,64
ML	0,21+/-0,06	0,19+/-0,08	0,80+/-0,11	0,39+/-0,02
GL	0,02+/-0,005	0,02+/-0,004	0,12+/-0,03	0,03+/-0,01

Fig. 1. Cell proliferation in the young rabbit cerebellum (sagittal sections). Newly generated cells, detected with Ki67 (A, red) and BrdU at 2-h (A, B, green; F, brown) or 5-day (G, brown) survival time, are concentrated in the SPL. Their subpial position is confirmed in double labeling with laminin (B, red), in semithin sections (C, arrowhead) and electron microscopy (D). (g) Bergmann glial endfeet; bv, meningeal blood vessel; p, pial cell; m, mitosis; bl, basal lamina. (E) Apoptotic figure in the SPL; ab, apoptotic bodies; a, arachnoid cell; sas, subarachnoid space; c, collagen. (H–J) Quantitative analysis of BrdU+ cells in the SPL, ML and GL at different survival times. 2 h, 2 hours; 5d, 5 days; (1i) single BrdU injection; (5i), five daily injections. Scale bars: 10 μm (A–C); 2 μm (D, E); 50 μm (F, G).

cells were arranged to form a single non-continuous layer (12.14 ± 3.39 BrdU+ nuclei/mm; Figs. 1F and 2M), irregularly covering the whole cerebellar surface. We will refer to this thin region which persists beyond puberty as the subpial layer (SPL), to distinguish it from the postnatal EGL (see below). Electron microscopy confirmed the occurrence of mitotic figures in the SPL, at the interface between the basal lamina of the pia mater and the ML (Fig. 1D), thus providing independent evidence (see Rakic, 2002) for cell proliferation at this level. Some figures with typical morphological signs of apoptotic cells were also detectable in the SPL (Fig. 1E).

Local cell proliferation was rare in cerebellar cortical layers outside the SPL (Fig. 1F). The cell density of BrdU+ elements after 2-h survival was 700 times higher in the SPL than in cortical tissue (Fig. 1I). The ANOVA for repeated measures revealed no significative reduction of the number of BrdU+ nuclei, but an interaction between time and their distribution in cellular layers considered, namely SPL, ML, GL ($F = 11.215$; $P = 0.005$). Furthermore, the one-way ANOVA in each cellular layer indicated a reduction of BrdU+ nuclei in the SPL between 2-h and 5-day survival time ($F = 8.699$; $P = 0.042$). No remarkable differences were observed in different medial–lateral or rostral–caudal extensions of the cerebellum, indicating a remarkable homogeneity of this process in the entire cerebellar cortex. Being cell proliferation of the SPL widely scattered over a large surface area and not concentrated within a discrete anatomical site (as is the case for the forebrain SVZ neurogenesis; see Peretto et al., 1999; Gage, 2000; Alvarez-Buylla and Garcia-Verdugo, 2002), we treated other animals with 5 daily injections of BrdU, in order to detect a larger

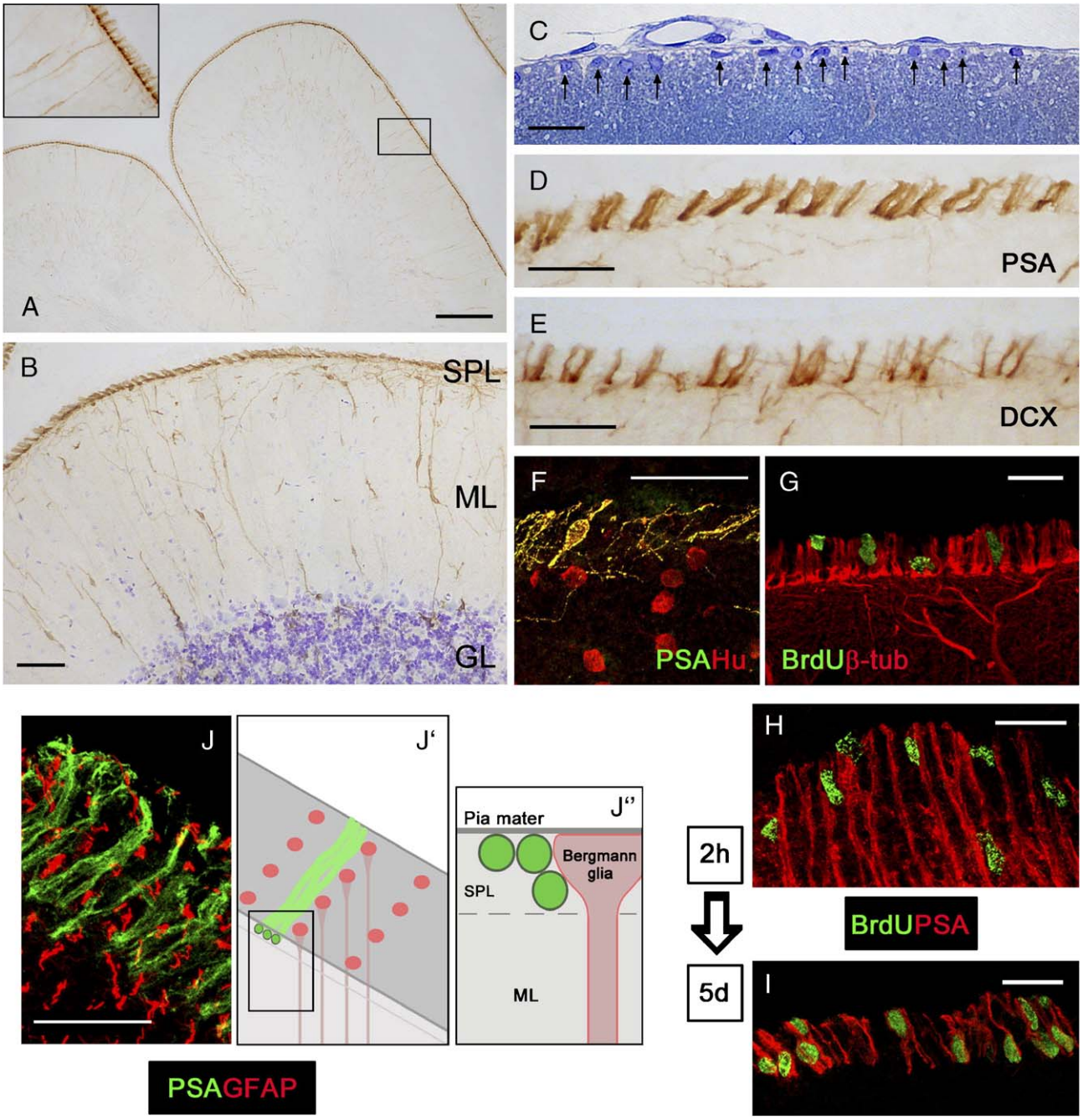

Fig. 2. Organization of the SPL in peri-puberal rabbits (sagittal sections). Immunocytochemistry for PSA-NCAM (A, B, D, brown; F, J, green; G–I, red) identify tangentially oriented chain-like structures in the SPL of the entire cerebellar cortex (A, B, D, F–J). Numerous PSA-NCAM+ cells are also detectable in the ML (B, cresyl violet counterstained). (C) Regularly arranged, subpial cells (arrows) in a semithin section. (E–G) Chains of cells in the SPL show antigenic features of neuronal precursors, being immunoreactive for doublecortin (DCX, E), HuC/D protein (Hu, F), and class III β-tubulin (β-tub, G). (H, I) These cells are newly generated: double staining with BrdU (green) and PSA-NCAM (red) at different postinjection stages (2 h and 5 days) shows local cell proliferation among chains in the SPL (H), whereas the newly generated cells become part of the chains in the subsequent 5 days (I). (J–J′) The SPL chains are oriented in a medial–lateral way, following rows of GFAP+ Bergmann glial endfeet. Scale bars: 200 μm (A); 50 μm (B); 20 μm (C–J).

population of newly generated cells. In animals which had received the same number of BrdU injections but were killed after 2 weeks, a remarkable decrease in newly generated cells was observed in the SPL, whereas many had survived in the ML and GL (Fig. 1H). In this case, the ANOVA for repeated measures revealed a highly significative interaction between time and distribution of BrdU+ nuclei in cellular layers ($F = 37.17$; $P = 0.000$) as well as a remarkable reduction in their number ($F = 92.76$; $P = 0.001$). The one-way ANOVA in each cellular layer indicated a significative reduction of BrdU+ nuclei in all layers considered, notably in the SPL (SPL, $F = 84.373$, $P = 0.001$; ML, $F = 12.96$, $P = 0.023$; GL, $F = 11.022$, $P = 0.029$). These data suggest that the cell genesis occurring in subpial position could be followed by displacement

through the cortical tissue, although only a small population actually survives after 2 weeks. The total number of BrdU+ cells/layer (Fig. 1H) as well as their percentage compared with the entire cell population in each layer was higher in the ML than in the granule layer at all survival times (Fig. 1J). It is important to note that cell density was similar in the two cortical layers (Fig. 1I), due to a larger extension of the ML.

In 6-month-old rabbits, the occurrence of dividing cells had dramatically decreased, even on the cerebellar surface, and in adult (1 and 2 years old) animals only scattered BrdU+ or Ki67+ nuclei were occasionally detected (not shown).

Newly generated neuronal precursors in the SPL form thousands of small chains

In order to explore the nature and arrangement of newly generated cells in the SPL, we performed immunocytochemistry by using antibodies raised against specific neurogenesis-associated molecules. Firstly, we detected the polysialylated form of the neural cell adhesion molecule (PSA-NCAM), a glycoprotein strictly associated to the entire population of adult-generated neuronal precursors in the hippocampus (Seki and Arai, 1991; Bonfanti et al., 1992) and SVZ (Bonfanti and Theodosis, 1994; Rousselot et al., 1995; Doetsch and Alvarez-Buylla, 1996; Petreanu and Alvarez-Buylla, 2002; Luzzati et al., 2003), required for their migration (Ono et al., 1994; Hu, 2000). Unlike the cerebellum of rodents after the EGL exhaustion, which lacks PSA-NCAM (Bonfanti et al., 1992, and this study; see Fig. 6), in rabbits, we found many immunoreactive cells, most of which were localized on the subpial surface (Figs. 2A, B, D). A remarkable number of PSA-NCAM+ cells with neuronal-like morphology were also present in the cortical tissue, most of which were localized within the ML (Fig. 2B; see below). A semiquantitative analysis of the relative amount of PSA-NCAM+ cells in 3-month-old rabbits indicated that 85% (898.33 ± 15.21 chains, namely 1796.67 ± 30.42 cells in 10 mm) of them are confined within the SPL, 12% (251 ± 11.60) in the ML, and only 3% (66 ± 3.00) in the remaining layers (Purkinje cell layer, inner granule layer and white matter).

Thus, the attention was focused on the SPL, where all the cells appeared as tangentially oriented, bipolar elements grouped to form chain-like structures (Fig. 2D), reminiscent of the chains of neuroblasts described in the SVZ of rodents (Lois et al., 1996) and rabbits (Luzzati et al., 2003; Ponti et al., unpublished). These chain-like structures were homogeneously present on the whole cerebellar extent in all animals in which there had been no damage to the cerebellar surface during dissection. About 7000 of these structures were present along the perimeter of a single representative sagittal section of the vermis (spaced about 10–20 μm from one another in 3-month-old animals; Figs. 2A, B, D), regularly arranged with a prevalent medial–lateral orientation. In GFAP/PSA-NCAM double stainings, they appeared in close contact and regular relationships with rows of Bergmann endfeet, contacting them transversely at the junction with the pia mater (Figs. 2J, J′, J″).

To establish their real nature as chains, these aggregates were analyzed with electron microscopy (Fig. 3). Small subpial cells (about 3–4 μm in diameter) sharing exactly the same pattern of the PSA-NCAM+ chain-like structures were detectable in sagittal semithin sections of resin-embedded lamellae (Figs. 1C, 2C, and 3C). The ultrastructural study revealed the typical cytology of neuroblasts (Lois et al., 1996; Jankovski and Sotelo, 1996; Doetsch et al., 1997; Peretto et al., 1997; Luzzati et al., 2003) (SVZ type A cells, Lois et al., 1996), with a large nucleus and a thin halo of electrondense cytoplasm, and confirmed the localization of these cells at the basal lamina/ML interface (Fig. 3). One or two, rarely three cell bodies were associated with differently sized processes containing the same type of cytoplasm, thus forming aggregates which were clearly recognizable from the surrounding axons and glia. Cerebellar coronal sections (longitudinal to these aggregates) revealed their identity as continuous, tangential chains of bipolar-shaped elements with leading and trailing processes (Fig. 3B). Further characterization was obtained by carrying out a serial ultrastructural reconstruction of two subpial tangential chains along a 21 μm tract of cerebellar surface (Figs. 3C–G). Due to the existence of many thin cell processes intermingled with cell bodies, a careful analysis involving 43 parasagittal levels was performed in order to follow the processes of individual cells. A very elongated bipolar neuroblast was entirely reconstructed within a chain (the cell colored in red in Fig. 3). The serial reconstruction showed that several long processes of SPL neuroblasts are closely associated with few cell bodies, thus forming very thin chains. The SPL chains were in direct contact with the glia limitants formed by the Bergmann endfeet and with the parallel fibers, rarely coming into direct contact with basal lamina. As already visible in light microscopy (see Figs. 2D, E, J), and confirmed by the ultrastructural reconstruction (Fig. 3), different chains can contact one another at some points to form a subpial network.

In addition to ultrastructural cytology, the neuronal nature of subpial cells was confirmed by immunoreactivity for the microtubule binding protein doublecortin (DCX), a marker specifically associated to neuroblasts and differentiating healthy neurons produced in adult neurogenic areas (Nacher et al., 2001; Brown et al., 2003; Rao and Shetty, 2004), the early neuronal marker class III β-tubulin (Menezes and Luskin, 1994; Peretto et al., 1997; Alvarez-Buylla and Garcia-Verdugo, 2002) and HuC/D protein (Goldman, 1997). As described for PSA-NCAM, staining for these markers also clearly revealed the tangential chains (Figs. 2E–G). The glial markers O4, Ng2, vimentin, and GFAP were used to evaluate the putative occurrence of cell precursors of the glial lineage in the SPL. After a careful search for colocalizations with BrdU+, no associations were found in either early- or late-generated cells (not shown). For these reasons, we conclude that cell genesis in the young rabbit SPL is devoted to the production of neuronal precursors.

Since cell proliferation and chains of neuroblasts are both in subpial position, we combined local cell proliferation markers (Ki67 and 2-h survival BrdU) and PSA-NCAM to understand their mutual relationships. Most of the locally dividing cells were interposed among the chains (Fig. 2H), whereas many

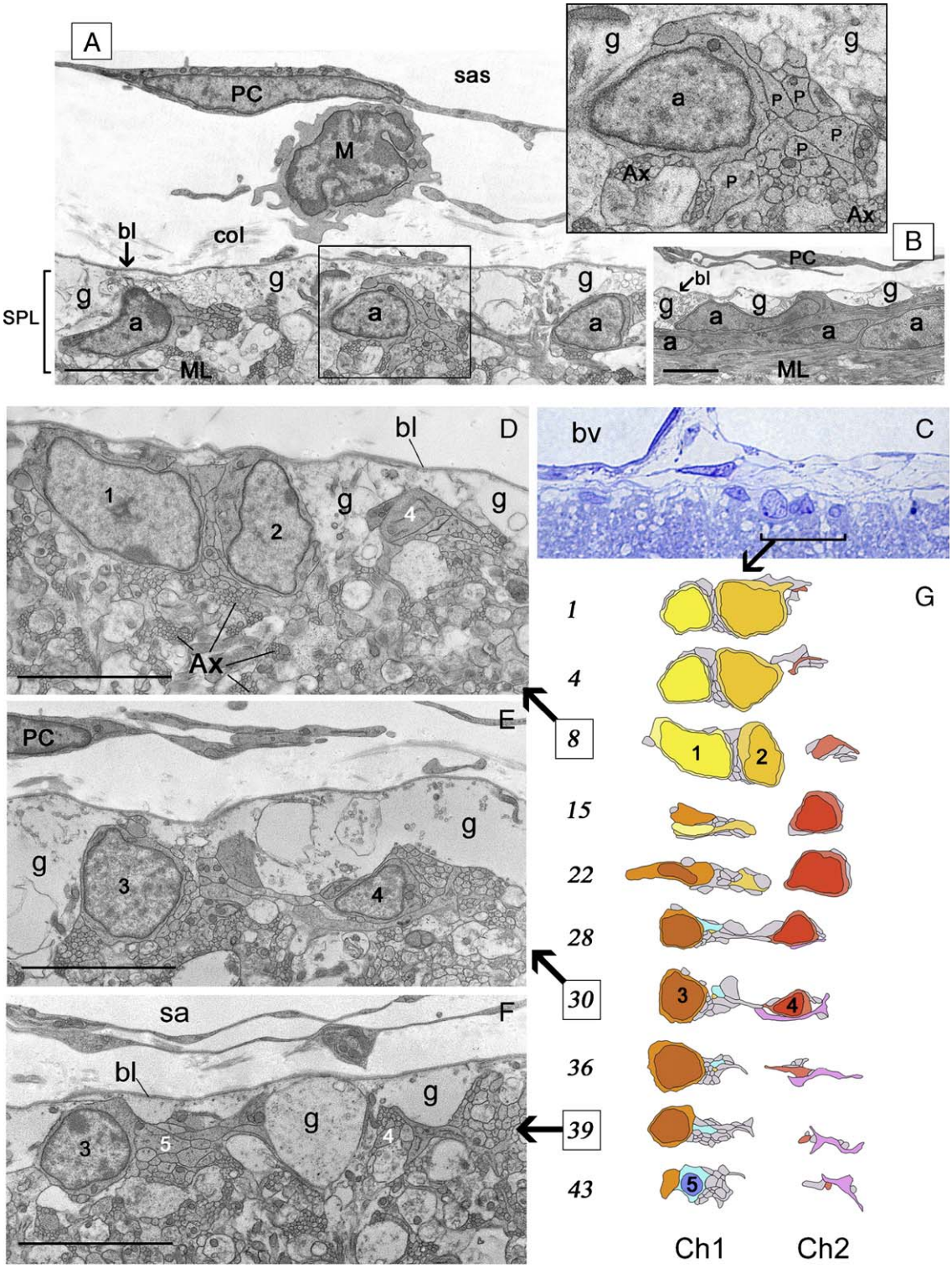

Fig. 3. Ultrastructure of rabbit SPL chains. Sagittal (A) and coronal (B) sections. Type A cells (a) with large nucleus and a thin halo of electrondense cytoplasm are regularly arranged in subpial position, separated from the basal lamina (bl) by glial endfeet (g). These cells are associated with large processes (P; A, inset) showing the same type of cytoplasm and distinguishable from axons (Ax) of the ML. In orthogonal views (B), these aggregates show features of tangential chains, formed by elongated bipolar-shaped cells. (C–G) Serial reconstruction of two subpial chains (Ch1 and Ch2; note that at the beginning they are fused in a single chain). (C) Semithin section at the beginning of the reconstruction. (G) Some representative levels of total 43 drawings. Each nucleated cell has a different color. Numbers in italic on the left are the levels (three of them are showed in the micrographs D–F). Numbers within the cell nuclei identify the 5 cells reconstructed, both in drawings and in micrographs. PC, pial cell; M, macrophage, sas, subarachnoid space; col, collagen; bv, blood vessel. Scale bars: 4 μm.

immunoreactive nuclei resided inside the chains in BrdU-treated animals which survived 5 days (Fig. 2I). Accordingly, the number of BrdU/PSA-NCAM double-labeled cells in the SPL progressively increased at subsequent survival times. This confirms that the SPL is made up of two cell compartments: actively dividing cells which do not yet express PSA-NCAM (Bonfanti and Theodosis, 1994; Rousselot et al., 1995), and chains of PSA-NCAM-immunoreactive cells containing the newly generated elements (with a 1/10 proportion, respectively). These compartments are part of the same population of newly generated cells forming a fragmented monolayer which is structurally different from the postnatal EGL.

Transition from EGL to SPL and postpuberal follow-up of the SPL

In the present study, we show that the proliferative capacity of the postnatal cerebellum in rabbits does not disappear as early as previously thought (Smith, 1963). The cerebellar EGL, although sharing features with the SVZ and hippocampus (Hatten, 1999), has so far been considered as a transient germinal zone destined to disappear after accomplishing granule cells genesis (Smith, 1963; Altman and Bayer, 1997). Yet, in the rabbit, the occurrence of the SPL does not simply seem to be the persistence of an EGL since important differences characterize its structure as well as ML cell composition throughout its existence.

In order to identify the transition time from postnatal EGL to peri-puberal SPL, we followed its histology, contents of proliferating cells and PSA-NCAM distribution in young rabbits at different postnatal stages (Fig. 4). Similarly to postnatal rodents (Dey et al., 1999, and this study, see below and Fig. 5), PSA-NCAM was absent in the proliferative EGL but present in the ML and granule layer as a diffuse reaction that reaches its high intensity at the limit between EGL and ML, in association with cells of the premigratory layer (Figs. 4D and 6).

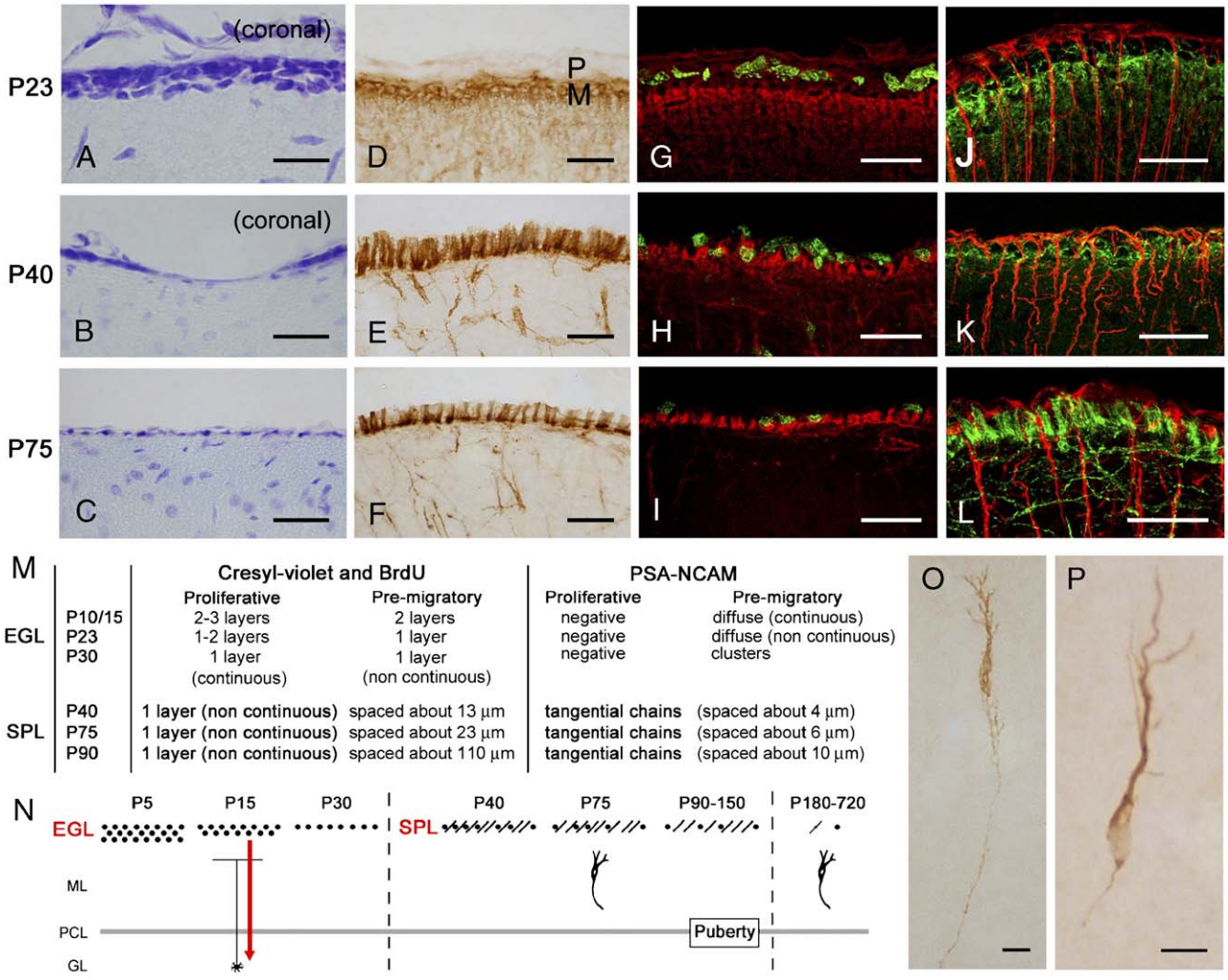

Fig. 4. Transition from EGL to SPL (A–M), and its further follow-up in the adult rabbit (N–P). Fragmentation of the proliferative layer (P) and its fusion with the premigratory layer (M) around P30 (summarized in M) is followed by the appearance of chains. The distance among proliferating cells and chains increases at subsequent postnatal stages (E, F, H, L–N). Cresyl violet (A–C), PSA-NCAM (brown, D–F), PSA-NCAM (red)/BrdU (green) (G–I), and PSA-NCAM (green)/GFAP (red) (J–L) stainings. (C–L) Parasagittal sections. (N) Follow-up of SPL and postpuberal neurogenesis in the rabbit cerebellum. Transition between EGL and SPL coincides with differences in the ML. Black dots, proliferating cells; black lines, chains. In older (1 year, O; 2 years, P) animals a SPL is no longer detectable, although some PSA-NCAM+ (O) and DCX+ (P) neuronal-shaped cells are detectable in the ML. Scale bars: (A–L) 20 µm; (O, P) 10 µm.

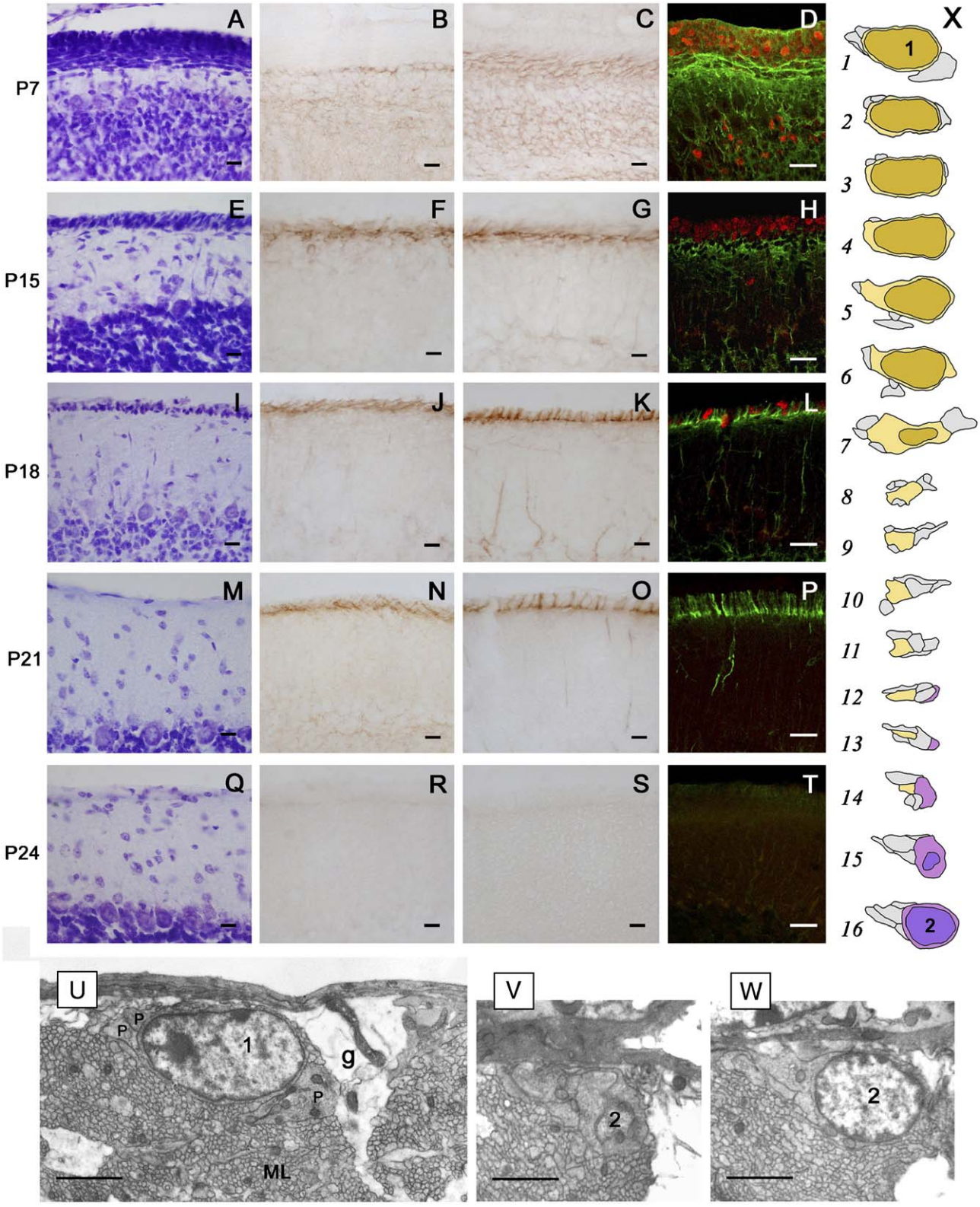

Fig. 5. Cellular/molecular features of the mouse EGL at the end of granule cell genesis. (A, E, I, M, Q) cresyl violet; (B, F, J, N, R) PSA-NCAM; (C, G, K, O, S) DCX; (D, H, L, P, T) Ki67 (red)/DCX (green) double staining. At early stages, characterized by a thick EGL (e.g., P7), PSA-NCAM, and DCX stainings are diffuse in the granule and molecular layers but absent in the EGL (B, C). Starting from P15, the immunoreactivity for these molecules is associated with tangentially oriented, subpial cells (F, G). At P18-P21, the PSA-NCAM- and DCX-positive cells form chains, although staining for PSA-NCAM is faint (J, K, N, O). At subsequent stages no immunoreactivity can be detected in the cerebellum (R–T). Detection of Ki67 shows that coexistence of cell proliferation and chains is limited to P18 (L), whereas only chains are detectable at P21 (P). (U–X) Ultrastructural reconstruction of a 16 μm tract of cerebellar surface in a 21-day-old mouse. (X) Drawings of a subpial chain-like aggregate; two nucleated cell bodies (indicated with numbers 1 and 2) and their processes are represented in color. Levels are indicated with italic numbers. (U–W) Micrographs of levels 1, 15, and 16, respectively. Scale bars: (A–T) 20 μm; (U–W) 2 μm.

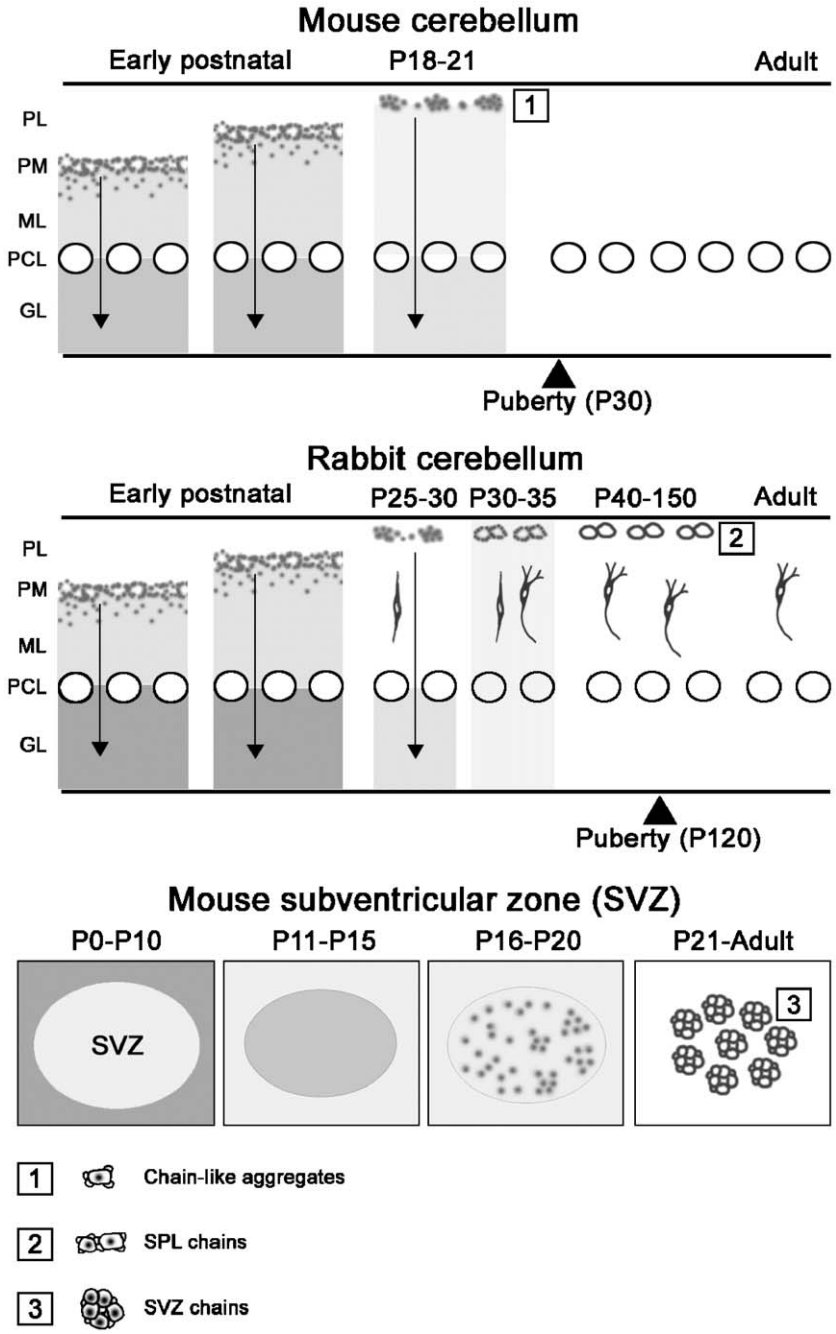

Fig. 6. Schematic representation of changes in PSA-NCAM distribution (grey) occurring at specific postnatal stages in persisting germinative layers of the brain and cerebellum of mouse and rabbit, compared to a similar pattern described in rodent SVZ (modified from Peretto et al., 2005). At early postnatal stages, PSA-NCAM shows a diffuse distribution in the regions located outside the germinative layers, being absent in the EGL proliferative layer (PL) of the cerebellum and in the forebrain SVZ. A stronger, punctate reaction is present on cells of the EGL premigratory layer (PM), both in mouse and rabbit cerebellum. At subsequent stages, corresponding to the end of granule cell genesis (arrows), PSA-NCAM reveals the fragmentation of the EGL in chain-like structures, which in the rabbit persist beyond puberty (arrowhead) as SPL chains, whereas in mouse, they completely disappear. Note that rabbit SPL chains occur in parallel with PSA-NCAM+ neuronal-like cells in the molecular layer (ML). A very similar pattern of chain formation is detectable in the forebrain SVZ. Numbers in squares indicate the different type of chain-like structures and chains, as revealed by electron microscopy (bottom).

This pattern was observed from P10 to P30, and later when the EGL was reduced to a single layer (P30-P40), PSA-NCAM staining firstly revealed chain-like structures at the border with the ML (Fig. 4E). After P40, no distinction between proliferative and premigratory layers was detectable, and the use of cell proliferation markers confirmed the fragmentation of proliferative EGL into a non-continuous layer, intermingled with the chains (Figs. 4H, I). This pattern was maintained up to 3–5 months of age, with a progressive increase in distance among chains and the consequent reduction in their number (Figs. 4C, F, I, L, M). Thus, the SPL spans from 1 to 5 months of age, persisting shortly beyond puberty (summarized in Figs.

4M, N). Bearing in mind that in all the species studied, the reduction of EGL to a monolayer is a crucial step which is thought to be followed by its disappearance (Fujita, 1967; Fujita et al., 1966; Altman, 1969; Rakic, 1971; Abraham et al., 2001), and that in rabbits, this stage coincides with the first appearance of tangential chains, the shift between EGL and SPL was fixed between P30 and P40 (Figs. 4M, N). Such a shift is reminiscent of the modifications occurring in the forebrain SVZ of rodents at the end of the first month of life, leading to formation of the rostral migratory stream chains from an homogeneous mass of neuronal precursors in the neonatal SVZ (Peretto et al., 2005; see Fig. 6).

From the sixth month of life, a typical SPL was no longer detectable (see Fig. 4N). At this age, only scattered KI67+ nuclei and PSA-NCAM+ cells were present at the cerebellar surface (not shown). In addition, some cells immunoreactive for DCX and PSA-NCAM were still detectable in the ML even in older animals (1- and 2-year-old rabbits; Figs. 4O, P), suggesting that a low level of cell genesis persists in the cerebellar cortex after the disappearance of a recognizable SPL.

Small chain-like aggregates in the mouse EGL at the end of granule cell genesis

At early postnatal stages (e.g., P7; see Fig. 5), the mouse EGL displayed morphological and molecular features similar to that of other species, including the rabbit. It was made up of several layers of cells (Fig. 5A), the PSA-NCAM staining being absent in the proliferative layer and present as a dense, intercellular reaction in the granule layer (Fig. 5B).

Towards the end of granule cell genesis (P15–P18), the EGL was firstly reduced to a monolayer of densely packed cells covering the whole cerebellar surface, as revealed by cresyl violet stainings (Figs. 5E, I). By using the markers PSA-NCAM and doublecortin in immunocytochemical stained specimens, some tangentially oriented cells (Fig. 5F) or chain-like stripes (Fig. 5G), respectively, were visible starting from P15.

A few days later, starting from P18, this layer became discontinuous (Fig. 5I). As the distance between cells progressively increased, some discrete clusters displaying a regular arrangement were visible in parasagittal sections. The pattern of immunostaining characterized by chain-like structures showing the same medio-lateral arrangement described in the rabbit became more evident at P18 (Figs. 5J, K). These structures were still detectable at P21 (Figs. 5N, O), when they were clearly distinguishable with anti-DCX antibodies, whereas the staining for PSA-NCAM was fainter and less well defined.

As previously described in literature (Fujita, 1967; Fujita et al., 1966), cell proliferation in the proliferative layer of the mouse EGL (Figs. 5D, H) had dramatically decreased at P18 (Fig. 5L), and no dividing cells were present from P21 onward (Figs. 5P, T).

An ultrastructural analysis carried out on parasagittal sections of the mouse cerebellar surface at P21 (Figs. 5U–X) revealed the existence of single neuroblasts oriented along a medial–lateral direction, forming small clusters with processes of other cells of the same type. A serial reconstruction of a single tract of one of these clusters confirmed that some neuroblasts tend to form small chains (Fig. 5Y). These chains were even smaller than those described in the rabbit SPL and did not involve several cell bodies at the same level, with each cell body being surrounded by a small number of processes. As observed in rabbits, even mouse chains were frequently adjacent to the Bergmann glia endfeet.

On examining the cerebellar surface at P24 and subsequent stages, no cell aggregates were observed in cresyl violet specimens (Fig. 5Q), and no PSA-NCAM or DCX immunoreactivities (Figs. 5R, S) were detectable, apart from some DCX+ chain-like structures, which were restricted to the surface of the ventral part of lamellae I and X, close to the fourth ventricle, up to P24–26 (not shown). This immunostaining had completely disappeared at P28. Thus, the persistence of mouse chain-like structures, and therefore an SPL-like structure, can be estimated in a very short time (4–5 days), without any overlapping proliferative activity.

Discussion

The postnatal follow-up of EGL is different in lagomorphs and rodents

Here, we show that at the end of the first month of life the classical morphology of the EGL in the rabbit cerebellum is replaced by a transitory germinal zone (SPL), characterized by active cell proliferation and production of neuroblasts, persisting beyond puberty. A remarkable feature of the SPL is the presence of chains of neuronal precursors morphologically and antigenically similar to those described in the forebrain SVZ (Lois et al., 1996; Jankovski and Sotelo, 1996; Doetsch et al., 1997; Peretto et al., 1997, 1999; Gage, 2000; Alvarez-Buylla and Garcia-Verdugo, 2002; Luzzati et al., 2003). We show that these chains in the rabbit SPL form one of the two compartments (dividing cells and chains) of the same population of newly generated cells appearing as a fragmented monolayer, which is structurally different from the postnatal EGL.

Both SPL compartments showed homogeneous topographical distribution throughout the cortical extension, thus excluding the possibility of a restricted area of the cerebellum being the source of newly generated cells and their reaching the entire surface area by chain migration. Indeed, no cell proliferation was detectable in the ependymal regions of the IVth ventricle. From the end of granule cell genesis (1st/2nd month of age) up to puberty (4th–5th month), the neurogenetic process in the SPL is remarkable. Then between the 5th and 6th month, it almost completely disappears. Throughout this period of time, the SPL is accompanied by the occurrence of numerous PSA-NCAM+ cells in the cortical tissue, particularly concentrated within the ML, thus suggesting that the persistent SPL is linked to differences concerning the subjacent layers (Ponti et al., unpublished). Among the mammalian species studied so far, neither the existence of a secondary germinal matrix similar to the rabbit SPL, nor the occurrence of cells expressing markers linked to structural plasticity (PSA-NCAM, see Bonfanti et al.,

1992) and neurogenesis (DCX) in the cerebellar cortex have been described. This suggests that the long-lasting occurrence of an actively proliferating SPL is specific to the rabbit. To investigate such a difference in detail, we re-examined the last phases of EGL exhaustion in the mouse to find that a fragmentation of the EGL premigratory layer does occur at the end of granule cell genesis, just before the EGL disappearance, leading to the formation of small chain-like aggregates. Nevertheless, in the mouse, the occurrence of these structures is limited to a very short period of time (4–5 days), followed by their complete disappearance after P21. No PSA-NCAM+ or DCX+ cells can be detected in the whole cerebellar cortex after this stage. Even the immunostaining which reveals chain-like aggregates in the mouse cerebellum (particularly concerning PSA-NCAM) is very faint, a fact that could explain how these structures had previously gone undetected. Thus, the fragmentation of the EGL appears to be a new finding representing a common pattern concerning EGL postnatal fate in different mammals. This fragmentation, as well as granule cell genesis as it is known in mammals, do follow a common pattern as indicated by a similar diffuse intercellular distribution of molecules not specifically associated to granule cell precursors in the early postnatal cerebellum of both species (Dey et al., 1999, and this study; see Fig. 6 and below). Nevertheless, substantial differences do exist in mice and rabbits after the end of granule cell genesis. First of all, the temporal window of chain persistence is very different (a few days in mice, more than four months in rabbits) and not comparable owing to the different developmental periods in the two species. Indeed, in all altricial species studied, the end of both EGL and granule cell genesis do occur before puberty whereas the rabbit SPL is still detectable beyond puberty. Secondly, the long-lasting rabbit SPL chains are formed by the close association of two-three cell bodies and many cell processes and strongly express plasticity-linked molecules, thus displaying true features of chains, despite being smaller than their counterpart in the forebrain SVZ (Lois et al., 1996; Jankovski and Sotelo, 1996; Doetsch et al., 1997; Peretto et al., 1997, 1999). On the other hand, the mouse chain-like structures are ill-defined aggregates faintly expressing PSA-NCAM and rapidly vanishing in a matter of days. Finally, and most importantly, the mouse chain-like structures occur at a stage when cell proliferation in the EGL is highly down-regulated (at P18) or it is already exhausted (at P21), whereas the rabbit SPL chains are continuously refilled with newborn cells.

These findings show that the postnatal fate of cerebellar EGL can vary remarkably if different mammals are concerned, thus suggesting that the persistence of secondary germinal zones should be re-evaluated in different species. For example, it has been suggested that ‘islands’ of EGL-like tissue can persist in humans, limited to some individuals, a fact that might be linked to the origin of medulloblastomas (Rubinstein, 1975). In this context, the rabbit can be considered an animal model to study late postnatal neurogenesis in a region of the mammalian CNS (the cerebellum) which is not endowed with similar processes in rats and mice.

The functional significance of a persistent SPL in rabbits remains at present obscure. The occurrence of PSA-NCAM+ cells with neuronal morphology in the ML could lead to the exclusion of protracted genesis of granule cells for the granule layer. Moreover, ectopic granule cells, whose existence has been described in this species (Spacek et al., 1973), have a different morphology and distribution. Further studies inferring the tracing of the progeny are requested to clarify the origin of these cells and their possible relation with the SPL. Indeed, some PSA-NCAM+ cells of the ML are still present in fully adult rabbits when the SPL is no longer active, also suggesting the existence of alternative sources (Ponti et al., unpublished).

The rabbit SPL shares features with the forebrain SVZ

The newly generated cells of the rabbit SPL share the ultrastructural (Lois et al., 1996; Jankovski and Sotelo, 1996; Doetsch et al., 1997; Peretto et al., 1997; Luzzati et al., 2003) and molecular (Bonfanti and Theodosis, 1994; Rousselot et al., 1995; Lois et al., 1996; Jankovski and Sotelo, 1996; Doetsch and Alvarez-Buylla, 1996; Doetsch et al., 1997; Peretto et al., 1997; Gage, 2000; Alvarez-Buylla and Garcia-Verdugo, 2002; Bernier et al., 2002; Petreanu and Alvarez-Buylla, 2002; Luzzati et al., 2003) features typical of SVZ type A cells (Lois et al., 1996), namely the progeny of neuronal precursors generated within the adult forebrain (Peretto et al., 1999; Gage, 2000; Alvarez-Buylla and Garcia-Verdugo, 2002). And yet the aggregation of SPL neuroblasts to form tangential chains is the most striking similarity with the adult brain neurogenetic area.

Compared to SVZ chains (Lois et al., 1996; Jankovski and Sotelo, 1996; Peretto et al., 1997, 1999; Alvarez-Buylla and Garcia-Verdugo, 2002), SPL chains are smaller and far more numerous, which matches with the remarkable amount of cell genesis detectable throughout the whole young cerebellum, despite low doses of BrdU used (Cameron and McKay, 2001). Moreover, as revealed by the ultrastructural serial reconstruction, neuroblasts of the SPL chains have very elongated leading and trailing processes, as confirmed by the fact that one or two cell bodies in a single transverse section are in contact with a large number of processes. These features, along with the absence of continuous glial structures as a substrate (the SPL chains are in contact with many Bergmann endfeet, but they cross them transversely), do suggest that, if they actually migrate, their displacement could not be fast, as described for chains of the forebrain rostral migratory stream (Lois et al., 1996). In this context, the functional role of chains in the SPL does remain speculative. Their orientation along the longitudinal axis of the folium is reminiscent of the tangential movement of granule cell precursors which has been demonstrated to occur in the premigratory layer of mice EGL and which is thought necessary for their appropriate allocation across parasagittal compartments (Komuro et al., 2001). Thus, SPL chains could have a role in the tangential displacement of newly born elements along the whole subpial surface.

Another intriguing feature shared by brain and cerebellum neurogenetic sites is the tendency of neuroblasts to assemble

into tangential chains at specific postnatal stages. This can represent a common pattern displayed by persisting germinative layers while adaptating to the maturing nervous system (see Peretto et al., 2005). Indeed, in mice SVZ, this transition does occur around the third postnatal week, in coincidence with the end of EGL and granule genesis in the cerebellum (Peretto et al., 2005). In both CNS regions, this stage is associated with dramatic changes in the anatomical and molecular environment surrounding the newly born cells, marking the end of postnatal neurogenesis and its shift to a neurogenetic process occurring within a mature nervous tissue (Peretto et al., 2005 and Fig. 6).

On the other hand, the importance of chain formation in the cerebellum seems to be quite different in mice and rabbits, being short and transitory in the former and long-lasting and well structured in the latter. This suggests that the persistence of a germinative layer reminiscent of (but not identical to) the postnatal EGL might be a very different feature in different mammals, which is worthwhile investigating in future studies as to its functional implications. Nevertheless, the transitory character of the rabbit SPL, which progressively reduces and virtually extinguishes its proliferative potential at increasing ages, indicates that it is different from brain neurogenetic areas persisting throughout life, suggesting that the SPL does contain a population of neuronal progenitors rather than stem cells. This assumption, although speculative, is also supported by the absence of astrocytic cell bodies within the germinative layer, an element which may be required to form a neural stem cell niche as is presently known to occur in the SVZ and hippocampus (Doetsch et al., 1997; Seri et al., 2004).

Acknowledgments

This work was supported by MURST (F.I.R.B.), Compagnia di San Paolo, Regione Piemonte and Università di Torino. We are very grateful to Ferdinando Rossi for reading the manuscript.

References

Abraham, H., Tornoczky, T., Kosztolanyi, G., Seress, L., 2001. Cell formation in the cortical layers of the developing human cerebellum. Int. J. Dev. Neurosci. 19, 53–62.

Altman, J., 1969. Autoradiographic and histological studies of postnatal neurogenesis: III. Dating the time of production and onset of differentiation of cerebellar microneurons in rats. J. Comp. Neurol. 137, 433–458.

Altman, J., Bayer, S.A. (Eds.), 1997. Development of the Cerebellar System. CRC Press, Boca Raton.

Alvarez-Buylla, A., Garcia-Verdugo, J.M., 2002. Neurogenesis in adult subventricular zone. J. Neurosci. 22, 629–634.

Bernier, P.J., Bédard, A., Vinet, J., Lévesque, M., Parent, A., 2002. Newly generated neurons in the amygdala and adjoining cortex of adult primates. Proc. Natl. Acad. Sci. U. S. A. 99, 11464–11469.

Bonfanti, L., Theodosis, D.T., 1994. Expression of polysialylated neural cell adhesion molecule by proliferating cells in the subependymal layer of the adult rat, in its rostral extension and in the olfactory bulb. Neuroscience 62, 291–305.

Bonfanti, L., Olive, S., Poulain, D.A., Theodosis, D.T., 1992. Mapping of the distribution of polysialylated neural cell adhesion molecule throughout the central nervous system of the adult rat: an immunohistochemical study. Neuroscience 49, 419–436.

Brown, J.P., Couillard-Despres, S., Cooper-Kuhn, C.M., Winkler, J., Aigner, L., Kuhn, H.G., 2003. Transient expression of doublecortin during adult neurogenesis. J. Comp. Neurol. 467, 1–10.

Cameron, H.A., McKay, R.D., 2001. Adult neurogenesis produces a large pool of new granule cells in the dentate gyrus. J. Comp. Neurol. 435, 406–417.

Dey, P.M., Gochfeld, M., Reuhl, K.R., 1999. Developmental methylmercury administration alters cerebellar PSA-NCAM expression and Golgi sialyltransferase activity. Brain Res. 845, 139–151.

Doetsch, F., Alvarez-Buylla, A., 1996. Network of tangential pathways for neuronal migration in adult mammalian brain. Proc. Natl. Acad. Sci. U. S. A. 93, 14895–14900.

Doetsch, F., Garcìa-Verdugo, J.M., Alvarez-Buylla, A., 1997. Cellular composition and three-dimensional organization of the subventricular germinal zone in the adult mammalian brain. J. Neurosci. 17, 5041–5046.

Fujita, S., 1967. Quantitative analysis of cell proliferation and differentiation in the cortex of the postnatal mouse cerebellum. J. Cell Biol. 32, 277–287.

Fujita, S., Shimada, M., Nakamura, T., 1966. H3-Thymidine autoradiographic studies on the cell proliferation and differentiation in the external and internal granular layers of the mouse cerebellum. J. Comp. Neurol. 128, 191–208.

Gage, F.H., 2000. Mammalian neural stem cells. Science 287, 1433–1438.

Goldman, S.A., 1997. Comparative strategies of subependymal neurogenesis in the adult forebrain. In: Gage, F.H., Christen, Y. (Eds.), Isolation, Characterization and Utilization of CNS Stem Cells. Springer-Verlag, Berlin, pp. 43–65.

Hatten, M.E., 1999. Central nervous system neuronal migration. Annu. Rev. Neurosci. 22, 511–539.

Hu, H., 2000. Polysialic acid regulates chain formation by migrating olfactory interneuron precursors. J. Neurosci. Res. 61, 480–492.

Jankovski, A., Sotelo, C., 1996. Subventricular zone-olfactory bulb migratory pathway in the adult mouse: cellular composition and specificity as determined by heterochronic and heterotopic transplantation. J. Comp. Neurol. 371, 376–396.

Kee, N., Sivalingam, S., Boonstra, R., Wojtowicz, J.M., 2002. The utility of Ki-67 and BrdU as proliferative markers of adult neurogenesis. J. Neurosci. Methods 115, 97–105.

Komuro, H., Yacubova, E., Yacubova, E., Rakic, P., 2001. Mode and tempo of tangential cell migration in the cerebellar external granule layer. J. Neurosci. 21, 527–540.

Lois, C., Garcìa-Verdugo, J.M., Alvarez-Buylla, A., 1996. Chain migration of neuronal precursors. Science 271, 978–981.

Lossi, L., Ghidella, S., Marroni, P., Merighi, A., 1995. The neurochemical maturation of the rabbit cerebellum. J. Anat. 187, 709–722.

Luzzati, F., Peretto, P., Aimar, P., Ponti, G., Fasolo, A., Bonfanti, L., 2003. Glia independent chains of neuroblasts through the subcortical parenchyma of the adult rabbit brain. Proc. Natl. Acad. Sci. U. S. A. 100, 13036–13041.

Menezes, J.R.L., Luskin, M.B., 1994. Expression of neuron-specific tubulin defines a novel population in the proliferative layers of the developing telencephalon. J. Neurosci. 14, 5399–5416.

Nacher, J., Crespo, C., McEwen, B.S., 2001. Doublecortin expression in the adult rat telencephalon. Eur. J. Neurosci. 14, 629–644.

Ono, K., Tomasiewicz, H., Magnuson, T., Rutishauser, U., 1994. N-Cam mutation inhibits tangential neuronal migration and is phenocopied by enzymatic removal of polysialic acid. Neuron 13, 595–609.

Peretto, P., Merighi, A., Fasolo, A., Bonfanti, L., 1997. Glial tubes in the rostral migratory stream of the adult rat. Brain Res. Bull. 42, 9–21.

Peretto, P., Merighi, A., Fasolo, A., Bonfanti, L., 1999. The subependymal layer in rodents: a site of structural plasticity and cell migration in the adult mammalian brain. Brain Res. Bull. 49, 221–243.

Peretto, P., Giachino, C., Aimar, P., Fasolo, A., Bonfanti, L., 2005. Chain formation and glial tube assembly in the shift from neonatal to adult subventricular zone of the rodent forebrain. J. Comp. Neurol. 487, 407–427.

Petreanu, L., Alvarez-Buylla, A., 2002. Maturation and death of adult-born olfactory bulb granule neurons: role of olfaction. J. Neurosci. 22, 6106–6113.

Rakic, P., 1971. Neuron-glia relationship during cell migration in developing cerebellar cortex: A Golgi and electron microscopic study in *Macacus* Rhesus. J. Comp. Neurol. 141, 283–312.

Rakic, P., 2002. Neurogenesis in adult primate neocortex: an evaluation of the evidence. Nat. Rev., Neurosci. 3, 65–71.

Rao, M.S., Shetty, A.K., 2004. Efficacy of doublecortin as a marker to analyse the absolute number and dendritic growth of newly generated neurons in the adult dentate gyrus. Eur. J. Neurosci. 19, 234–246.

Rousselot, P., Lois, C., Alvarez-Buylla, A., 1995. Embryonic (psa) N-CAM reveals chains of migrating neuroblasts between the lateral ventricle and the olfactory bulb of adult mice. J. Comp. Neurol. 351, 51–61.

Rubinstein, L.J., 1975. The cerebellar medulloblastoma: its origin, differentiation, morphological variants, and biological behavior. In: Vinken, P.J., Bruyn, G.W. (Eds.), Handbook of clinical neurology, vol. 18. North-Holland-Elsevier, pp. 167–193.

Sanchez-Villagra, M.R., Sultan, F., 2001. The cerebellum at birth in therian mammals, with special reference to rodents. Brain Behav. Evol. 59, 101–113.

Seki, T., Arai, Y., 1991. Expression of highly polysialylated NCAM in the neocortex and piriform cortex of the developing and the adult rat. Anat. Embryol. 184, 395–401.

Seri, B., Garcia-Verdugo, J.M., Collado-morente, L., McEwen, B.S., Alvarez-Buylla, A., 2004. Cell types, lineage, and architecture of the germinal zone in the adult dentate gyrus. J. Comp. Neurol. 478, 359–378.

Smith Jr., K.R., 1963. The cerebellar cortex of the rabbit. An electron microscopic study. J. Comp. Neurol. 121, 459–483.

Spacek, J., Parizek, J., Lieberman, A.R., 1973. Golgi cells, granule cells and synaptic glomeruli in the molecular layer of the rabbit cerebellar cortex. J. Neurocytol. 2, 407–428.